ELSEVIER

Available online at www.sciencedirect.com

ScienceDirect

Progress in Natural Science: Materials International 21(2011) 122−126

Progress in Natural Science: Materials International

www.elsevier.com/locate/pnsc

Fabrication and characterization of TiO_2-based dye-sensitized solar cells

Takeo OKU, Nariaki KAKUTA, Kengo KOBAYASHI, Atsushi SUZUKI, Kenji KIKUCHI

Department of Materials Science, The University of Shiga Prefecture, Shiga 522-8533, Japan

Received 10 February 2011; accepted 15 April 2011

Abstract: Dye-sensitized solar cells TiO_2 with were fabricated. The phase composition and microstructures of the solar cells were examined by X-ray diffractometry and transmission electron microscopy, and the energy levels of the present solar cells were also discussed. The results show that a solar cell mixed with xylenol orange and rose Bengal shows a higher conversion efficiency compared to solar cells with a single dye. An introduction of amorphous TiO_2 layers results in an improvement of the conversion efficiency.

Key words: solar cell; TiO_2; dye; porphyrin; microstructure

1 Introduction

Electrical energy storage systems have been developed[1], and solar cells are one of the good candidate clean energy devices because of no production of carbon dioxide causing global warming[2−3]. Although silicon (Si) solar cells have high conversion efficiency and a long lifetime, their production processes are complicated and expensive.

Dye-sensitized solar cells, based on the concept of photo-sensitization of wide band-gap mesoporous oxide semiconductors[4], are now in a state of advanced development. This technology has been established as a promising low-cost photovoltaic concept[5], and has featured applications that can be colored and are lightweight. However, dye-sensitized solar cells have a short lifetime due to leakage and vaporization of the electrolytes. Therefore, the studies of solidification of dye-sensitized solar cells have been performed[6−7], and organic dyes without noble metals are expected as low-cost dyes.

The purpose of the present work is to investigate electrical and optical properties of dye-sensitized solar cells (DSSC), with an amorphous TiO_2 layer to introduce electrons at trap levels in acceptor and donor levels. The effects of organic dyes addition such as protoporphyrin IX (PPIX), xylenol orange (XO) and rose Bengal (RB) to dye-sensitized solar cells were fabricated and characterized.

2 Experimental

The schematic illustrations of the present solar cells are shown in Fig.1. Nanocrystalline TiO_2 photoelectrodes were prepared using the following procedure. TiO_2 powder was dispersed in an aqueous solution (1 mL) in a mixture of acetylacetone (0.02 mL, Shigma Aldrich Inc.) with Triton X−100 (0.01 mL, ICN Biomedicals Inc.) with polyethylene glycol (0.2 g, PEG#20 000, Nacalai Tesque Co. Ltd.)[8−9]. The TiO_2 paste was coated on pre-cleaned FTO by the squeegee method. After the TiO_2 coating, the FTO substrate was sintered for 30 min at 450 °C, and the prepared titanium isopropoxide (TTIP) solution dropped on the substrate. After that, the substrate was sintered for 60 min at 180 °C. The TTIP solution was prepared by mixing TTIP (0.3 mL, Sigma Aldrich Co. Ltd.), acetilaceton (0.08 mL), ethanol (0.64 mL) and PEG# 20 000 (0.2 g, Nacalai Tesque Co. Ltd.). The TiO_2 electrodes were dissolved into the solved organic dyes such as, protoporphyrin (Aldrich Co. Ltd.), xylenol orange and rose Bengal solutions (Tokyo Chemical Industry Co. Ltd.) in distilled water, methanol or ethanol (Nacalai Tesque Co. Ltd.)[10−12]. Bellfine (0.1 g, Air Water Inc.) and Denka black (0.02 g, Denki Kagaku Kogyo Co. Ltd.) as carbon was dispersed in the distilled water (0.8 mL) and ethanol (0.4 mL) with sodium carboxymethyl cellulose (0.012 g, Tokyo Chemical Industry Co. Ltd.)[13]. The carbon paste was applied on indium tin oxide (ITO, Geomatec Co. Ltd.) as

Corresponding author: Takeo OKU; Tel: +81-749-28-8368; E-mail: oku@mat.usp.ac.jp

an opposite electrode by the squeegee method. The heat treatment of the carbon on the ITO substrate was carried out at 180 °C for 30 min. The electrolyte fabricated in a mixture of iodine (0.05 g I_2, Wako Co. Ltd.), lithium iodide (0.09 g LiI, Wako Co. Ltd.), ethylene carbonate (0.41 g, Shigma Aldrich Inc.), propylene carbonate (0.5 mL, Shigma Aldrich Inc.) and polyacrylonitrile (0.17 g, Shigma Aldrich Inc.) was agitated and heated at 80 °C[14]. The dye-sensitized solar cells were assembled by putting the electrolyte between the adsorbed dye materials at the TiO_2 layer on the FTO glass substrate and the carbon film on the ITO substrate.

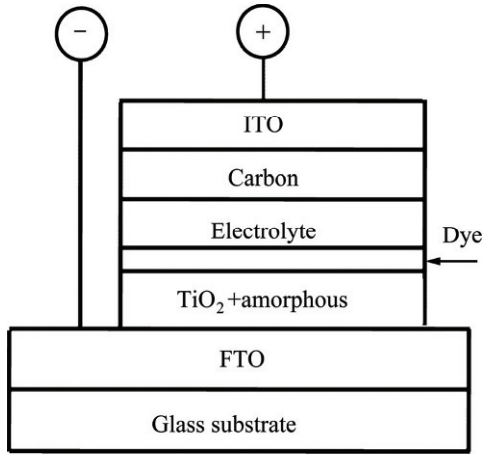

Fig.1 Structures of dye-sensitized solar cells with dyes

The current density−voltage (J−φ) characteristics (Hokuto Denko Corp., HSV−100) of the solar cells were measured both in the dark and under illumination at 100 mW/cm^2 by using an AM 1.5 solar simulator (San-ei Electric, XES−301S) in N_2 atmosphere. The solar cells were illuminated through the side of the FTO substrates, and the illuminated area was 0.16 cm^2. The optical absorption of the solar cells was investigated by means of UV-visible spectroscopy (Hitachi U−4100). The microstructures of the thin films were investigated by wide X-ray diffractometry (XRD, PHILIPS X'Pert-MPD System) with CuK_α radiation operating at 40kV and 40mA, scanning electron microscopy (SEM, Hitachi S-3200N), energy dispersive X-ray analysis (EDX, EMAX−5770W) and transmission electron microscopy (TEM, Hitachi H−8100).

3 Results and discussion

Measured cell performance of DSSCs is summarized as Table 1. Experimental parameters of open circuit voltage (φ_{oc}), short circuit current (J_{sc}), fill factor and conversion efficiency (η) are listed in Table 1. A normal DSSC with PPIX provided an efficiency of 2.3×10^{-3}.

A TEM image and an electron diffraction pattern of the DSSC with PPIX are shown in Figs.2(a) and 2(b), respectively. The TEM image indicates TiO_2 nanoparticles with sizes of 20~60 nm, and the electron diffraction pattern shows 101, 103 and 200 reflections of a tetragonal TiO_2 anatase phase. A high-resolution electron microscopy (HREM) image of an interface of TiO_2 nanoparticles is shown in Fig.2(c). The interface is directly connected in atomic scale, which would results in good carrier transport between TiO_2 nanoparticles. A HREM image of surface of the TiO_2 nanoparticle is shown in Fig.2(d), and the TiO_2 nanoparticle is covered by a 2 nm thick PPIX layer with an amorphous structure.

Table 1 Measured parameters of DSSCs

Sample	φ_{oc}/ V	J_{sc}/ (mA·cm^{-2})	Fill factor	η/ %
PPXI	0.091	0.088	0.29	2.3×10^{-3}
XO + RB without amorphous TiO_2	0.36	0.60	0.56	0.12
XO + RB with amorphous TiO_2 layer	0.33	0.83	0.58	0.16

Figure 3 shows an energy level diagram of the present DSSC with PPIX. φ_{oc} of the present DSSC would be related with the energy gap (E_g) between HOMO of PPIX and conduction band of TiO_2. The control of the energy gap is important for improving the efficiency. The light irradiation causes charge-separation at PPIX, and the electrons are transferred to conductive band of TiO_2. The holes at HOMO level of PPIX lead to conversion of I^- to I^{3-} in the electrolyte, and I^- reduced the oxidized porphyrin to porphyrin with normal valence.

The measured J−φ curves of DSSC with or without an amorphous TiO_2 layer are shown in Fig.4. It can be seen that the current density of DSSC with an amorphous TiO_2 layer was higher than that of DSSC without an amorphous TiO_2 layer. The cell performance is summarized in Table 1. The current density is improved from 0.6 to 0.83 mA/cm^2. The other parameters are almost the same. As a result, the conversion efficiency is improved from 0.12 % to 0.16 %.

Figure 5 shows the measured optical absorption of DSSC with an amorphous TiO_2 layer compared to that without an amorphous TiO_2 layer. An optical absorption peak of TiO_2 around 360 nm is increased by introducing the amorphous TiO_2 layer.

Figure 6 shows XRD patterns of TiO_2 layers prepared from the TTIP solution as a function of temperature. No peak of an anatase phase is observed when annealing at 250 °C. The small peaks of the anatase phase are observed after annealing at 350 °C. The diffraction peaks of TiO_2 (P25) are shown for comparison with the amorphous TiO_2.

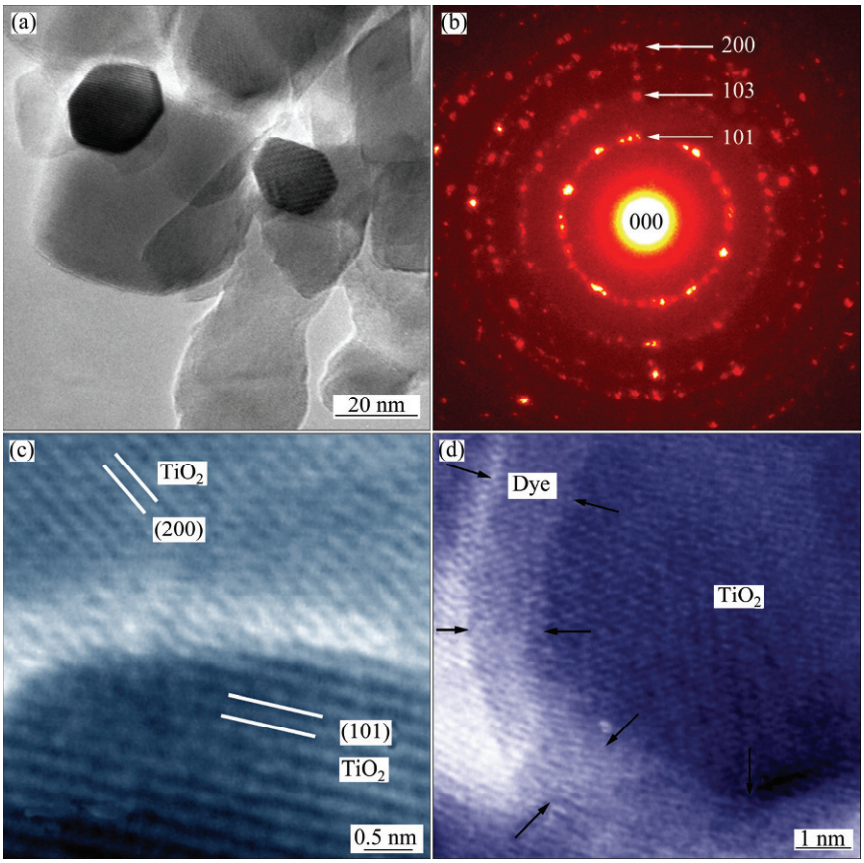

Fig.2 TEM image (a) and electron diffraction pattern of TiO_2 DSSC with protoporphyrin (b), HREM images of interface (c) and surface (d) of TiO_2 nanoparticles

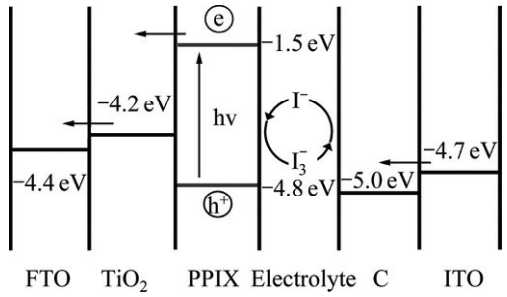

Fig.3 Energy level diagram of present DSSC with PPIX

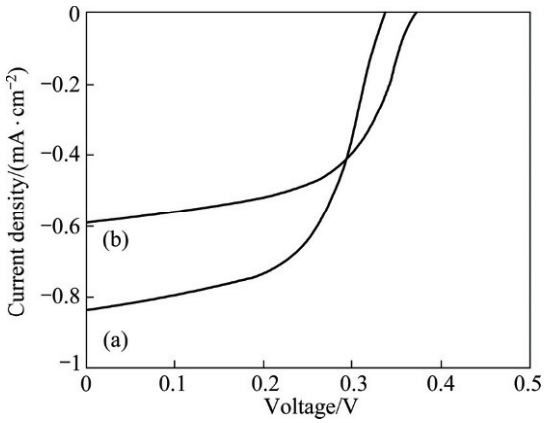

Fig.4 Current density—voltage curves of DSSCs with (a) or without (b) amorphousTiO_2 layer

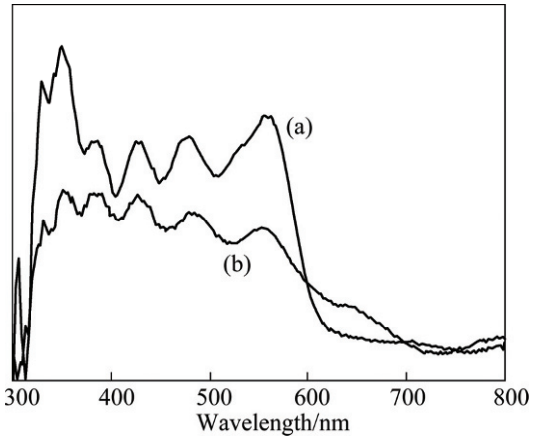

Fig.5 Optical absorption of DSSCs with (a) or without (b) amorphousTiO_2 layer

Figure 7 shows a TEM image and an ED pattern of the amorphous TiO_2 layer. The amorphous TiO_2 layer around the TiO_2 nanoparticle is observed in the TEM image. As shown in Fig.7(b), the EDS pattern indicates 101 and 103 reflections of the polycrystalline coagulation of TiO_2 with a tetragonal anatase structure. The diffuse ring of an amorphous phase is also observed, which indicates that the structure of the TiO_2 layer is a mixture of anatase and amorphous phases.

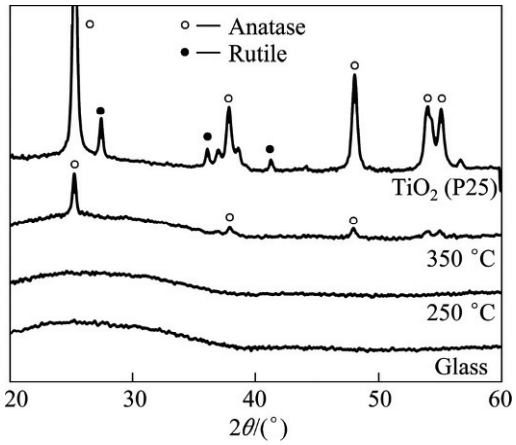

Fig.6 XRD diffraction patterns of TiO_2 layers as function of temperatures

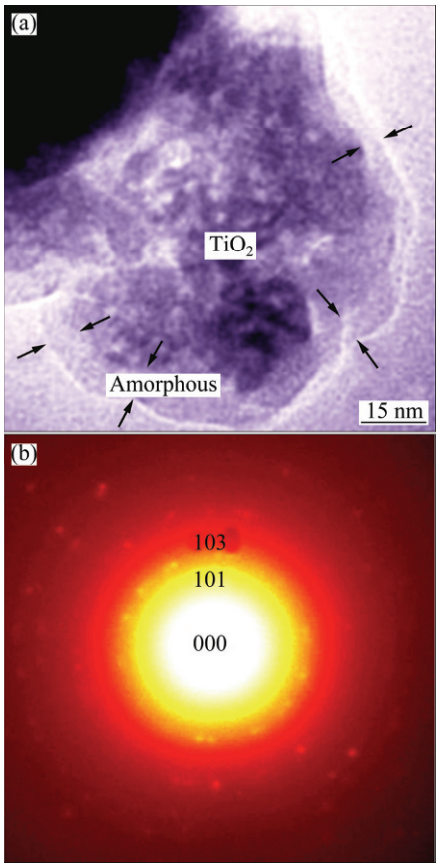

Fig.7 TEM image (a) and ED pattern (b) of amorphous TiO_2 layer

An energy level diagram of DSSC with the amorphous TiO_2 layer is shown in Fig.8. The values of HOMO and LUMO were calculated by Gaussian03 (B3LYP/6−31G*). An energy barrier would exist at the semiconductor metal interface. The electronic charge generation is caused by light irradiation from the FTO substrate side. The TiO_2 layer or amorphous TiO_2 layer receives the electrons from the dye, and the electrons are trapped by several trap levels of the amorphous TiO_2. The electrons are transported to an FTO electrode through the TiO_2 layer, and electrons are transferred to the outside circuit, and flow through the carbon electrode. Then, electrons return to the electrolyte by oxidation-reduction reaction. The improvement of the present solar cells is due to the introduction of the amorphous TiO_2 electrode, and this structure should be investigated further. The carrier recombination would be a main cause for low conversion efficiency. The improvement of the conversion efficiency can be expected by improving the charge separation and the electronic charge transfer.

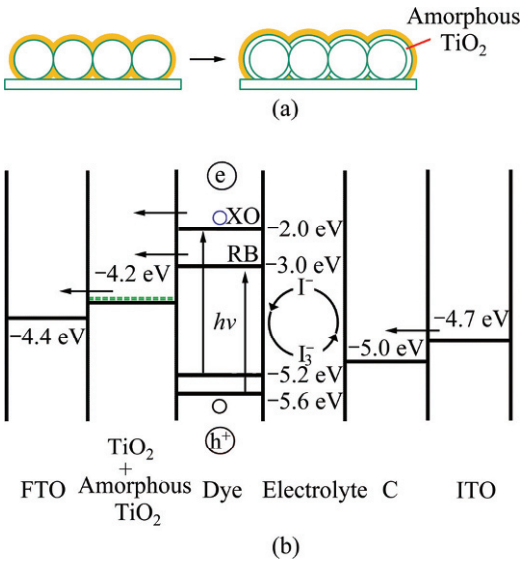

Fig.8 Schematic diagram (a) of TiO_2 electrode with amorphous TiO_2 layer and energy level diagram (b) of present DSSC with amorphous TiO_2 layer

The improvements of the conversion efficiency by coating materials on TiO_2 have been reported. The insulator oxides such as Al_2O_3 or SiO_2 on TiO_2 have been introduced for DSSCs [15]. These oxides suppress carrier recombination by reverse transfer of electrons in the cells. In the present study, DSSCs with amorphous TiO_2 layers on TiO_2 were fabricated, and the amorphous TiO_2 would attract electrons because of many trap levels in the acceptor and donor levels. In addition, the effectiveness of carrier separation is high because of large contact area. Further improvement would be possible by introducing nanoparticles as light harvesting materials[16−17].

4 Conclusions

1) Amorphous TiO_2 was introduced into DSSC with mixed xylenol orange and rose Bengal. The optical absorption peak of TiO_2 around 360 nm was increased by introducing the amorphous TiO_2 layer. Diffraction spots of the anatase phase and a diffuse ring from the amorphous phase were observed.

2) The proposed energy diagram showed that the amorphous TiO_2 would attract electrons at several trap levels in the TiO_2 layers. In addition, the carrier separation is high, which would be due to large contact area. As a result, the current density is improved from 0.60 mA/cm^2 to 0.83 mA/cm^2, and the conversion efficiency is improved.

References

[1] YUE W, ZHOU W. Crystalline mesoporous metal oxide[J]. Prog Nat Sci, 208, 18: 1329−1338.

[2] GREEN M A, EMERY K, KING D L, et al. Solar cell efficiency tables (version 28)[J]. Prog Photovolt Res Appl, 2006, 14: 455−461.

[3] OKU T, TAKEDA A, NAGATA A, et al. Fabrication and characterization of fullerene-based bulk heterojunction solar cells with porphyrin, $CuInS_2$, diamond and excision-diffusion blocking layer[J]. Energies, 2010, 3: 671−685.

[4] CHEN H, CONG T N, YANG W, et al. Progress in electrical energy storage system: A critical review[J]. Prog Nat Sci, 2009, 19: 291−312.

[5] DURR M, BAMEDI A, YASUDA A, et al. Tandem dye-sensitized solar cell for improved power conversion efficiencies[J]. Appl Phys Lett, 2004, 84: 3397−3399.

[6] MURAI S, MIKOSHIBA S, HAYASE S. Influence of alkyl dihalide gelators on solidification of dye-sensitized solar cells[J]. Sol Energy Mater Sol Cells, 2007, 91: 1707−1712.

[7] SCHMIDT-MENDE L, BACH U, HUMPHRY-BAKER R, et al. Organic dye for highly efficient solid-state dye-sensitized solar cells[J]. Adv Mater, 2005, 17: 813−815.

[8] LEWIS L N, SPIVACK J L, GASAWAY S, et al. A novel UV-mediated low-temperature sintering of TiO_2 for dye-sensitized solar cells[J]. Sol Energy Mater Solar Cells, 2006, 90: 1041−1051.

[9] NAZEERUDDIN M K, KAY A, RODICIO I, et al. Conversion of light to electricity by cis-X2bis(2,2'-bipyridyl-4,4'-dicarboxylate) ruthenium (II) charge-transfer sensitizers (X = Cl-, Br-, I-, CN-, and SCN-) on nanocrystalline titanium dioxide electrodes[J]. J Am Chem Soc, 1993, 115: 6382−6390.

[10] PRADHANA B, BATABYALA S K, PAL A J. Vertically aligned ZnO nanowire arrays in rose bengal-based dye-sensitized solar cells[J]. Sol Energy Mater Sol Cells, 2007, 91: 769−773.

[11] KAKUTA N, OKU T, SUZUKI A, KIKUCHI K, KIKUCHI S. Fabrication and characterization of mixture type dye-sensitized solar cells with organic dyes[J]. J Ceram Soc Jpn, 2009, 117: 964−966.

[12] MATSUBARA T, ICHIKAWA Y, ARAMAKI K, et al. The use of xylenol orange in a dye-sensitized solar cell[J]. Sol Energy Mater Sol Cells, 2005, 85: 269−275.

[13] IMOTO K, TAKAHASHI K, YAMAGUCHI T, et al. High-performance carbon counter electrode for dye-sensitized solar cells[J]. Sol Energy Mater Sol Cells, 2003, 79: 459−469.

[14] ILEPERUMA O A, DISSANAYAKE M A K L, SOMASUNDERAM S, et al. Photoelectrochemical solar cells with polyacrylonitrile-based and polyethylene oxide-based polymer electrolytes[J]. Sol Energy Mater Sol Cells, 2004, 84: 117−124.

[15] PALOMARES E, CLIFFORD J N, HAQUE S A, et al. Control of charge recombination dynamics in dye sensitized solar cells by the use of conformally deposited metal oxide blocking layers[J]. J Am Chem Soc, 2003, 125: 475−482.

[16] NAGATA A, OKU T, KIKUCHI K, et al, ŌSAWA E. Fabrication, nanostructures and electronic properties of nanodiamond-based solar cells[J]. Prog Nat Sci, 2010, 20: 38−43.

[17] PARK N G, KANG M G, RYU K S, et al. Photovoltaic characteristics of dye-sensitized surface-modified nanocrystalline SnO_2 solar cells[J]. J Photo-Chem Photobiol A, 2004, 161: 105−110.